SEPKA 2016

A NUMERICAL AND ANALYTICAL STUDY ON OPTIMIZATION AND EFFICIENCY OF STRUCTURAL FORMS BY TWO-OUTRIGGER IN TALL BUILDINGS

Bahram Marabi* & Abdul Kadir Marsono

Department of Structure and Material, Universiti Teknologi Malaysia, 81310 UTM Johor Bahru, Johor, Malaysia

*Corresponding Author: *bahrab.marabi@gmail.com*

Abstract: The selection of a suitable structural system and resist lateral loads in tall buildings plays an important role in structural design. The increase of the heights in the high-rise buildings will be limited because of exceed drift due to lateral loads. The outrigger systems always have been the best choice to limit the lateral deflections in slender buildings. This paper presents analytical and numerical methods to determine optimum location of the outriggers through the height of the building. Optimization and efficiency of the outriggered structural systems were examined in the reduction of the top drift. In the analytical method was used an idealized model as Two- Dimensional (2D) due to horizontal loads. In this regard, Three-Dimensional (3D) building frames were simulated as numerical method by Abaqus/CAE program. Two types conventional forms of the outrigger systems were considered as lateral resisting systems. The numerical models were utilized two outriggers as forms of (a) and (b). Pushover analysis was conducted under uniformly lateral load that was distributed throughout the height. The obtained results by the 2D analytical method shows that the model of the form (a) was optimized when the second outrigger located at 0.58H from the top of the structure while the first outrigger was fixed at the top, in the form (b) was optimized where the outrigger levels were placed at 0.31H and 0.69H, from the top of the building. The results of the 3D modelling by Finite Element Analysis (FEA) indicated that in the form (a) in which the first outrigger is fixed at the top and the second outrigger is optimized at 0.55H from the top of the model. In this way, two outrigger levels of the form (b) were optimized at 0.29H and 0.62H from the top of the structure. The efficiency of the optimized two forms of the outrigger systems in the reduction of the lateral drift at the top of the building by numerical modelling were determined; the efficiency of the outriggers system form (b) is 42% higher than optimized model of the form (a). The 3D Finite Element Analysis (FEA) method for use in the initial design of an outrigger structural system in tall buildings is recommended because of reliable results in compared to the 2D theoretical analysis in order to an optimum design of tall buildings structure.

Keywords: *Outrigger systems, tall buildings structure, FEA method, lateral resistance system, pushover analysis*

1.0 Introduction

1.1 Overview Considerations

Tall buildings behave compared to short and middle buildings is different in carrying lateral loads. Selection an appropriate structural system to resist horizontal loads, always engineers have been involving in this problem. Tall buildings structure is known as a cantilever structure which has merely flexural behavior. For this reason, lateral deflections are significant in the design of the flexural components. The performance of the tall buildings structural utilizes the outrigger systems, able to obviate this problem. The outrigger systems lead to the enhancement of the effective depth of flexural stiffness in lateral load resisting system in the tall building structure. The outrigger structural system resists rotation and overturning moments of the building, compared to a conventional structure without an outrigger. Tall buildings structure development involves several different factors such as stiffness, strength, ductility, light weight, technology and economics. In the meantime, stiffness has been the primary governing factor. Lateral deflection plays a significant role in the design procedure of the structure. Outrigger frame systems were improved by using outriggers to core-frame systems to tie the core to the peripheral columns via outrigger beam. This paper investigated slender buildings structure were equipped two-outriggers in order to optimize the lateral resistance structure system and minimized horizontal roof displacement. Tall buildings structure utilizes outrigger systems, have enhanced the lateral stiffness of the structure without changed the component sizes and increased mass of the building. Slender buildings structure or narrow tall building involved a central shear wall core as lateral resistance system. The structure equipped outrigger systems for coupling the core with the external columns. Thus, the outrigger structural systems include the main core, outrigger beams, and peripheral columns. An outrigger as deep beam that is occupied one or two-story, and also it be duplicated at one or few levels of the structure, that shown in Figure 1 illustrates this concept.

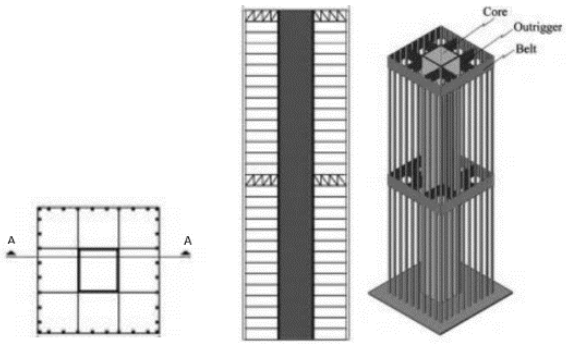

Figure 1: Outriggered frame system(Günel and Ilgin, 2014)

1.2 Literature Review

The optimum location of the second outrigger while the first outrigger was fixed at the top of the structure is analyzed by an analytical simple method in order to the preliminary design of the tall buildings' shear walls. The second outrigger has placed at the optimum location when the top displacement of the building was minimized under lateral loads. In this research, the optimum location of the second outrigger was obtained at 0.577H from the top of the structure. Two parametric diagrams were provided for optimum levels of the outriggers considering properties and stiffness ratio of the elements of the outrigger structural systems (Hoenderkamp, 2008). The optimum location of the outrigger was investigated in the shear walls frame. They have used one and two outriggers in the considered frames.

They were modeled and with and without changed of the components sizes considered frames using Etabs program and analyzed. Effect of reduction of the cross section was obtained from the analysis of the results when one outrigger was located at the top and another at the soft story. Obtained results were showed that single outrigger was optimized at 0.53H from the top of the structure. In this regard, for two outriggers in which one was fixed at the top and second was optimized at 0.7H from the top of the model, optimum locations for two outriggers through the height were optimized at 0.67H and 0.33H from the top of the building (Alpana, 2015). A 50-story building was investigated to obtain the optimum location of the outrigger in tall buildings structure subjected to earthquake loads. Response spectrum analysis was conducted, lateral displacement and inter-storey drift was determined.

Results of this study have shown that the structure was optimized when the outrigger is located at ranges of (0.52-0.56)H from the top of the building (Herath *et al.*, 2009). By using 'n' number of outriggers were applied at outrigger levels through the height of the building, the optimum location of them can be given nearly by the following formula; 1/(n+1), 2/(n+1) … n/(n+1) (Smith and Coull, 1991). The drift index limit value, norm, and practice of designers in different countries are in the following range, 1/1000 to 5/1000. This variable depends on the weight and height of the building that has been specified and recommended by design building codes (Ghosh *et al.*, 1996). A sixty-four RC story building with the ratio of 6:1 height-to-width of the building was investigated to examine the optimum location of the outriggers, and to decrease the wind load response. The outrigger position changes in the building's height are examined through numerical software to get the natural frequency and eigenvectors in the wind load path.

According to the ASCE 7-02 code, the along-wind responses were identified, though, the across-wind responses were computed, by considering the processes of the wind tunnel data due to aerodynamic load. Outcomes of the study revealed that the optimum location of the outriggers was between 1/3 to 2/3 height (Samat *et al.*, 2008). Static and dynamic behavior of reinforced concrete tall building with central shear core walls by

using the outrigger systems was investigated. In this study, the 3D structural model is conducted with flexural rigidity ratio range of (0.25 to 2.0) EIO/EI. Optimum outrigger location is obtained from the range of 0.975-0.40 (Hs/H), from the top of the building (Kamath *et al*., 2012). A static analysis due to wind load was investigated and was observed that the lateral deflection has reduced by 37% when the outrigger located at the top, and it was reduced up to 61% when it was located at a middle height and the base bending moment reduced by 95% in this location. The dynamic analysis subjected to earthquake load, results was indicated that lateral drift has been reduced by 34% in the middle height, and it was reduced by 64% when the outrigger was located at the 0.975H (Fawzia and Fatima, 2010). They have presented a parametric study on the optimization and parameters affecting position outriggers and behavior of the structure were investigated.

General analysis of shear walls with a pair of the rigid outrigger and a heavy beam in the desired position in height is provided. They have offered a parametric model behavior. Their results showed that the best location was 0·4 - 0·6 height of the structure where is minimized top drift of the building. This method is not recommended a substitute for the finite element method, only an initial solution identify of outrigger levels and to determine the outrigger size in the preliminary design procedure. Optimal location of the outrigger and the factors influencing their position was also examined (Zeidabadi *et al*., 2004). Formulae were developed for approximating the optimum location of the outriggers to reduce the drift at the top of the buildings. They were developed by using various regressions analysis to the relative effects of mix compatibility analyses up to four outriggers. The quick hand solutions by the formula for optimum location of outriggers and to obtain top drift and moment in the structure were investigated. However, their detailed formula is obtained only for idealized structures that are uniform with height. they were provided a useful practical objective in a guide to behavior, and estimation of the forces and deformation, while, practically no structure uniform with height (Smith and Salim, 1983).

2.0 Materials and Methods

2.1 Analytical Study

The method of analysis for a two-outrigger structure will be used a simplified analytical model that was separated into three superposition models as illustrated in Figure 2(a). Based on the superposition rule, all steps are considered simplest forms. The model to be included; bending moment diagram of the central core without the outrigger under outer lateral loads Figure 2(b), restoring moment diagram of first outrigger at (x_1) Figure 2(c), restoring moment diagram of second outrigger at (x_2) Figure 2(d), (x_1) and (x_2) measured from the top of the model. Resulting in reduced bending moment diagram due to the restoring moments of the outriggers effects, Figure 2(e), (Smith and Coull, 1991).

Moment-area method is used to obtain the core rotation at the outrigger levels 1 and 2, respectively

$$\theta_1 = \frac{1}{EI}\int_{x_1}^{x_2}\left(\frac{wx^2}{2} - M_1\right)dx + \frac{1}{EI}\int_{x_2}^{H}\left(\frac{wx^2}{2} - M_1 - M_2\right)dx \quad (1)$$

$$\theta_2 = \frac{1}{EI}\int_{x_2}^{H}\left(\frac{wx^2}{2} - M_1 - M_2\right)dx \quad (2)$$

where;

EI is flexural rigidity of the core, H is height of the core, W is intensity of lateral load (W/H unit.), x_1, x_2 are distance of outriggers 1 and 2 from the top of the structure respectively and M_1, M_2 are restraining moments on the core due to outriggers levels respectively.

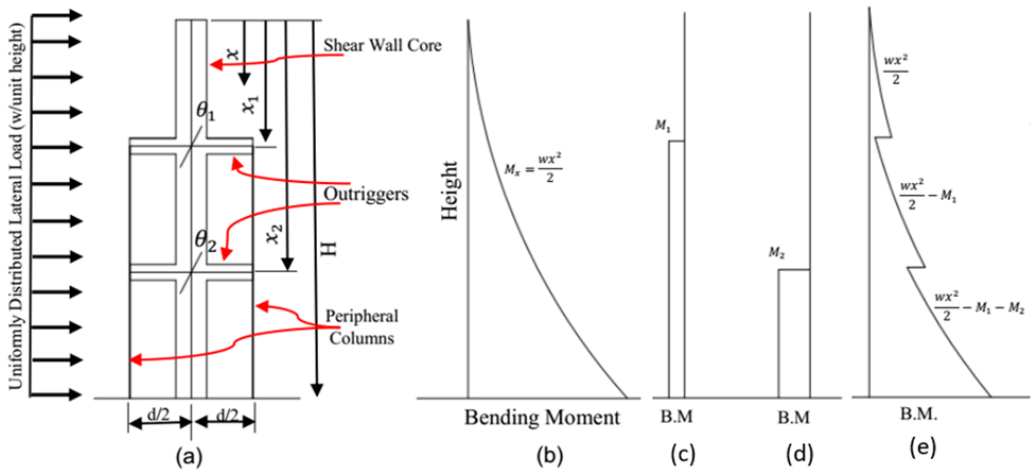

Figure 2: (a) Two-outrigger analytical model, (b) bending moment diagram under external load, (c) and (d) restoring momemt M_1 and M_2, (e) reduced bending moment diagram due to outriggers

The rotations of the outriggers at the points of connection to the core, includes two components: bending rotation of outrigger's beam due to external columns forces at end of the outriggers and another is outrigger rotation due to axial deformation of the external columns. The rotation of the outrigger at level 1 can be expressed as:

$$\theta_1 = \frac{2M_1(H-x_1)}{d^2(EA)_c} + \frac{2M_2(H-x_2)}{d^2(EA)_c} + \frac{M_1 d}{12(EI)_o} \quad (3)$$

And the rotation of the second outrigger at level 2 is:

$$\theta_2 = \frac{2(M_1+M_2)(H-x_2)}{d^2(EA)_c} + \frac{M_2 d}{12(EI)_o} \quad (4)$$

where;
$(EA)_c$ is axial rigidity of columns, $(EI)_o$ is effective flexural rigidity of the outrigger and $(d/2)$ is horizontal distance from centroid of the core to the columns.

Equating expressions (1) and (3) and similarly, (2) and (4) for the rotation of the core and the outriggers, by solving simultaneous equations above mentioned, the restraining moments applied to the central core due to the outriggers at levels 1 and 2 will be obtained values of the M_1 and M_2. In this manner, with varios assumptions consideration existing moment in the core at distance (x) from the top of the building which is shown in Figure 2(c) generrally can be expressed as:

$$M_x = \frac{wx^2}{2} - M_1 - M_2 \quad (5)$$

Thus,
M_1 is included only for $x > x_1$ and
M_2 is included only for $x > x_2$
The forces in the columns due to the outrigger action are:
$\pm M_1/d$ for $x_1 < x < x_2$ and
$(M_1 + M_2)/d$ for $x \geq x_2$
The maximum moment in the outriggers is then
$(M_1.b) / d$ for level 1 and
$(M_2.b) / d$ for level 2,

Where
b is the net length of the outrigger.

2.2 Analysis Latrral Diflection at the Top of the Structure

A general expression for horizontal deflections throughout the height, under uniform lateral load without any restraining moment, can be derived as:

$$\Delta_0 = \frac{w}{EI}\left[x^4 - 4H^3x + 3H^4\right] \tag{6}$$

In order to optimizing the top drift, the lateral deflection at the top of the structure without any restraining moment in Equation (Eq. 6), can be expressed as:

$$\Delta_0 = \frac{wH^4}{8EI} \tag{7}$$

While the lateral deflection due to restraining moment at throughout the height of the core is:

$$\Delta_R = \frac{1}{2EI}\left[M_1(H^2 - x_1^2) + M_2(H^2 - x_2^2)\right] \tag{8}$$

The total lateral deflection by combination of the equations (Eq. 7) and (Eq. 8), due to restraining moments at x_1 and x_2:

$$\Delta_T = \Delta_0 - \Delta_R = \frac{wH^4}{8EI} - \frac{1}{2EI}\left[M_1(H^2 - x_1^2) + M_2(H^2 - x_2^2)\right] \tag{9}$$

2.3 Optimum Locations for Two-Outrigger Structural Systems

In terms of conceptual analysis, for adding each outrigger to the vertical cantilever structure only one compatibility equation is necessary. So, with a two-outrigger structure requiring a solution of two compatibility equations because of two degrees indeterminacy. In this regards, the equations of the rotation of the core and the outriggers at the outrigger levels can be solved simultaneously. subsequently, the compatibility equations for the rotations at the outrigger levels are set up and solved simultaneously to obtain the values to M_1 and M_2 (Günel and Ilgin, 2014). According to the Equation (Eq. 9), the first phrase, represents horizontal deflection at the top of the core as a free vertical cantilever under the external lateral load and so, second phrase, represents the reduction in the top deflection due to the outrigger restraining moments as M_1 and M_2. The assessment of the optimum location of the outriggers to minimize the top deflection of the structure will be achieved by maximizing the drift reduction in Equation (Eq. 9). Following the procedure from the analysis of a two-outrigger structure, the second phrase of the Equation (Eq. 9) is maximized by differentiating with respect to

first, x_1, and then x_2 and equating to zero (Smith and Coull, 1991). Consequently, when the outriggers are located throughout the height of the core, the two-outrigger structural system is optimized, if the outrigger levels were placed at; $x_1 = 0.31H$ and $x_2 = 0.69H$, from the top of the model. Accordingly, the outrigger's restraining moments of two outrigger levels on the lateral drift at the top of the building, when one outrigger is located at the top of the building as $x_1 = 0$, the optimum location of second at x_2 is obtained by differentiating the second phrase of the equation (Eq. 9) with respect to x_2 and equating to zero. Thus, $x_2 = 0.58H$, from the top of the structure.

2.4 Efficiency Two-Outrigger Structural Systems

Efficiency of the tall buildings structure using a two-outrigger system in the reduction of lateral drift at the top of the building due to uniformly lateral distributed load through of the height and decrease base moment for two conventional forms based on the analytical results described as follows;

1. The first type model of two outrigger levels in which one outrigger is located at the top of the structure and the other outrigger located at the optimum place as type (a), in the reduction of the lateral drift at the top of the structure by 92% /(EIC).

2. The second type model of two outrigger levels in which both of outrigger are located at the optimum places through the height as type (b), in the reduction of the lateral drift at the top of the structure by 96% /(EIC).

3. For model of the type (a), in which one outrigger located at top and other located at the optimum place, 83% of the total restoring moment comes from the lower outrigger.

4. For model of the type (b), in which two outrigger levels were located at the optimum locations, 64% of the total restoring moment comes from the lower outrigger

2.5 Numerical Study

In this present research, inspired by the analytical method above mentioned, and promote 2D analytical models to 3D modeling analysis with consideration of the various assumptions, to enhance reliable results in the lateral load resisting system of tall buildings structure. For this purpose, a numerical method to Three-Dimensional (3D) building frames modeling is considered. The building frames that are equipped with two levels outrigger braced system as a lateral resistant system in the tall buildings. In this research, two types conventional models of the outrigger structural systems are used. First type model of the two-outriggered frame system in which, one outrigger is located at the top of the structure and another is placed at through the height of the building, as tyep (a) Figure 3. The second type model of the two-outriggered frame system while, two outrigger levels are located at through the height of the structure, type (b) Figure 3.

A central shear wall core is considered as a comparative cantilever structure which unemployed the outrigger system, type (c) Figure 3. The models that are simulated 3D two-outriggered frame systems and a central core alone are illustrated in Figure 3.

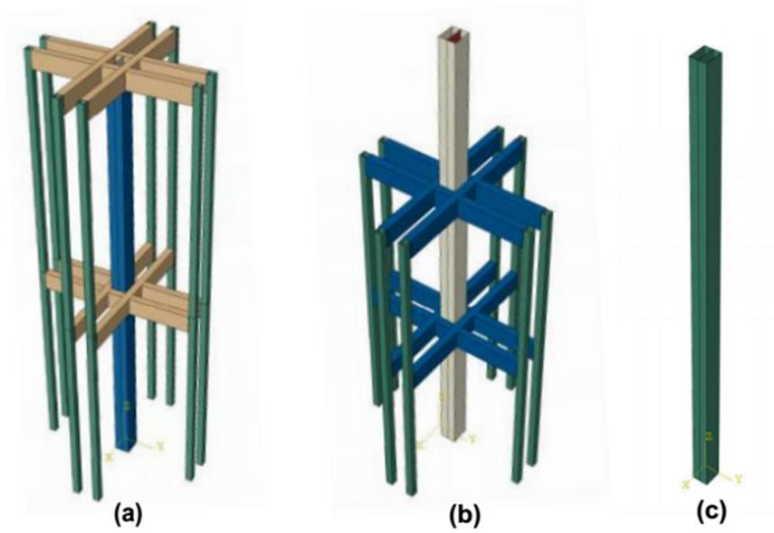

Figure 3: The 3D models of the two-outrigger structural frame systems; (a) First type models in which, one outrigger is fixed at the top and another located at through the height, (b) Second type models in which, both outriggers are located through the height, (c) a free standing core

2.6 Numerical Simulation Models and Analysis

The models consist a main core as central shear walls, outrigger beams, and peripheral columns. The model's element section sizes are considered as; the main core element is used double rectangular profile by 101.6×44.45×1.2 mm, the outrigger elements is used by 101.6×44.45×1.2 mm and square profile for columns is used by 38.1×38.2×1.2 mm. The type of the cross sections by shell element are considered in Abaqus /CAE 6.11 program. Meshing and elements type is conducted by using the linear, reduced-integration, quadrilateral shell element (S4R). The element shape for mashing is selected at the parts of the models which are simulated that shown in Figure 4.

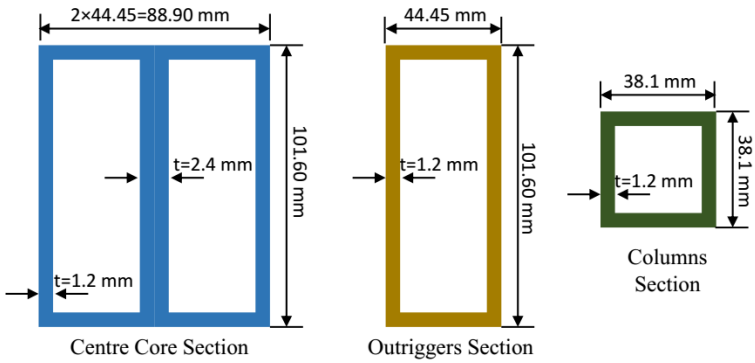

Figure 4: Profiles Size of the components which are used in the models

Whereas, boundary conditions and correlation of the structure's compounds, have a significant role in the simulation and results of the numerical analysis.For this reason, in the simulation of the models is conducted with high accuracy. Boundary condition of the core element is fixed to the base as a main cantilever member. The outriggers as horizontal components are merged connections on the core as fixed connection and are pinned to the peripheral columns at the other end, by using MPC technique constraint pin. The exterior columns have simply connected to the base as vertical members propose carrying axial loads. The overall dimension of the models is considered contains the height is 2550 mm, the width is 938.1 mm (centre-to-centre of the peripheral columns). Aspect ratio of the height-to-width in the models is respected by 2.72, that have been used in all models illustrated (See Fig. 3). The aim of pushover analysis is to evaluate performance of the structural by assessing stiffness and deformation demands in design seismic. Results of the pushover analysis include drift, inter story drift, deformations between elements and connection and inelastic element deformations with respect to a yield value. In this way, the models by force –controlled pushover analysis are carried out. The models are pushed in monotonically increasing order until target displacement is reached or structure goes to fail. Based on ATC-40 (ATC, 1996), FEMA- 273 (FEMA-273, 1997) and described in FEMA-356 (FEMA-356,

2000) Figure 5, average values for members of models are compared. Nonlinear static analysis (Pushover) is performed and nonlinear deformations considered that are selected in the steps of loading and boundary conditions of the analyzing. Simulation of the frame elements is modeled with first-order 3D aluminum material elements (AL), in which the nonlinear static deformation is allowed.

The characteristics elastic stiffness, yield strength and yield displacement of the pushover curve depend on the lateral force distribution. The uniform distribution generally leads to pushover curve with higher elastic stiffness, higher yield strength, and lower yield displacement compared to all other distributions (Goel, 2005).

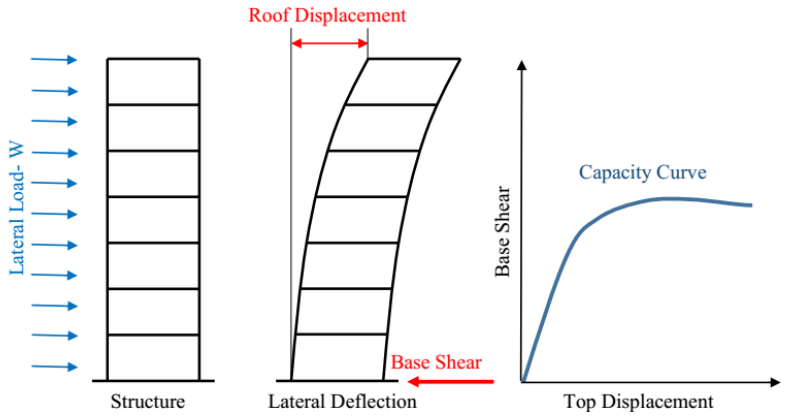

Figure 5: Pushover analysis method based on FEMA-356

The materials properties are taken by a real material mechanical tensile test which has been done in structures Laboratory are demonstrated in Table 1. Based on the engineering and true stress-strain values relationship of three specimens in conformance with *ASTM E 8 – 04* (Standard, 2004), the elasticity modulus $E = 68356.78$ Mpa, while Poisson's ratio is $\nu = 0.33$, are used.

Table 1: Engineering material characteristics result at the mechanical tensile Tests

Specimen	Load at Yield Zero Slop (N)	Tensile Strain at Yield Point (mm/mm)	Tensile stress at Yield Zero Slop (N/mm^2)	Extension at Yield Zero Slop (mm)	Maximum Load (N)	Tensile Strain at Maximum Load (mm/mm)	Tensile Stress at Maximum Load (N/mm^2)	Extension at Maximum Load (mm)	Modulus (Mpa)
S_1	2521.66	0.00445	168.11	0.58488	3047.58	0.08831	203.17	6.62694	68356.78
S_2	2372.76	0.00447	158.18	0.56829	2949.61	0.09394	196.64	7.13363	64535.49
S3	2243.76	0.00433	149.58	0.55872	2808.12	0.09022	187.21	6.96686	64368.95

Loading are carried out by using uniformly lateral load with intensives $W = 36\,(KN/m^2)$ for linear mode and $W \geq 36\,(KN/m^2)$ up to collapse for yield mode. The ultimate loading is performed in order to plastic mode that were distributed throughout the height of the models. The type of loads considered (W) were fixed for all types of the models loading, these loads based on force control demand were estimated that were yielded of the models.

2.7 Numerical Analysis and Optimization

According to the aims of the study which are investigated the horizontal drift values at the top of the building. In this regards, two different types of models are considered as type (a) and (b) that each of them two outriggers is equipped. Modeling and simulations were conducted under similar conditions. Pushover analysis subjected to uniformly distributed lateral loading were performed.

The first model of type (a), (see Fig. 3) in which, one outrigger location is fixed at the top of the structure and the second outrigger was moved its situations from the top downward to the base of the model. For determine optimum location of the second outrigger while an outrigger distancing $(x_1 = 0)$ is fixed and second outrigger distance ($x_2 = ?$) was placed at levels of $0.53H$, $0.54H$, $0.55H$, $0.56H$, $0.57H$, $0.58H$, $0.59H$, $0.60H$, $0.61H$ and $0.62H$ from the top of the structure. Following the definitions and assumptions built models, the models of type (a) is analysed under uniform lateral load with intensive $W = 36\,(KN/m^2)$ which distributed through the height. In this type of models,*10* positions were considered for the second outrigger location which are described above mentioned. The obtained results show that a second outrigger position where located at $0.55H$ from the top of the structure provided minimum lateral drift value at the top of the model by *34.55* mm. The numerical results of the type (a) are illustrated in Table 2.

The second model of type (b), (see Fig. 3) in which, both outriggers were located through the height of the central core of the building. The internal spacing of the outriggers and their distances from the top of the building were considered by x_1 and x_2. Based on the formula $1/(n+1)$, $2/(n+1)$ … $n/(n+1)$, (Smith and Coull, 1991) for internal spacing of two outriggers and distances from the top of the structure are 1/3 and 2/3 times of the height. In this analysis 5 models of type (b) were considered that their situations were palced at $(x_1 - x_2)$, by $(0.29 - 0.62)H$, $(0.31 - 0.64)H$, $(0.33 - 0.67)H$, $(0.35 - 0.68)H$ and $(0.37 - 0.70)H$. Three different models of the type (b) were conducted where one model was placed at internal spacing of two outrigger was $0.36H$, as by $(0.32 - 0.68)H$ and others were placed at internal space of two outriggers is $0.38H$, as by $(0.27 - 0.65)H$ and $(0.35 - 0.73)H$.

Analysis of the type (b) models was conducted under a similar uniform lateral loading that was distributed through the height of the models by $W = 36\,(KN/m^2)$. The

nonlinear static pushover analysis results were obtained based at the outrigger levels that are described above by the models of the type (b) results of this part illustrated in Table 3.

Table 2: Numerical results of the 3D two-outriggered structural frames of the models of type (a)

Outriggers Position	Outriggers Location H%	Distance From the Top x1 x2	Uniform Loading W	Base Shear F	Top Displacement d	Drift D%	Stiffness K	Natural Frequency Mode 1-x F	Natural Frequency Mode 2-y F	Base Moment	Top Rotation S%	Rotational Stiffness K
mm	H%	mm	KN/m2	N	mm	%	N/mm	Cycle/time	Cycle/time	N.mm	mm/mm	N.mm
x1	0	0	36	7106.22	34.72	1.36156863	204.67224	19.098	15.115	4081.33	0.00308	1325107.1
x2	0.53	1351.5										
x1	0	0	36	7115.32	34.62	1.35764706	205.52629	19.164	15.155	3994.69	0.00316	1264142.4
x2	0.54	1377										
x1	0	0	36	7125.33	34.55	1.35490196	206.23242	19.214	15.185	3923.53	0.00323	1214715.2
x2	0.55	1402.5										
x1	0	0	36	7134.14	34.58	1.35607843	206.30827	19.249	15.204	3944.48	0.00332	1188096.4
x2	0.56	1428										
x1	0	0	36	7144.79	34.61	1.3572549	206.43716	19.266	15.212	3754.69	0.00339	1107578.2
x2	0.57	1453.5										
x1	0	0	36	7153.9	34.76	1.36313725	205.8084	19.265	15.205	3707.58	0.00348	1065396.6
x2	0.58	1479										
x1	0	0	36	7164.62	34.9	1.36862745	205.28997	19.251	15.194	3615.96	0.00355	1018580.3
x2	0.59	1504.5										
x1	0	0	36	7174.16	35.13	1.37764706	204.21748	19.218	15.169	3530.87	0.00364	970019.23
x2	0.6	1530										
x1	0	0	36	7184.31	35.41	1.38862745	202.8893	19.168	15.132	3471.03	0.00373	930571.05
x2	0.61	1555.5										
x1	0	0	36	7194.18	35.76	1.40235294	201.17953	19.103	15.084	3403.28	0.00383	888584.86
x2	0.62	1581										

Table 3: Numerical results of the 3D two-outriggered structural frames of the models of type (b)

Outriggers Position	Outriggers Location H%	Distance From the Top x1 x2	Uniform Loading W	Base Shear F	Top Displacement d	Drift D%	Stiffness K	Natural Frequency Mode 1-x F	Natural Frequency Mode 2-y F	Natural Frequency Mode 3-z F	Base Moment	Top Rotation S%	Rotational Stiffness K
mm	H%	mm	KN/m2	N	mm	%	N/mm	Cycle/time	Cycle/time	Cycle/time	N.mm	mm/mm	N.mm
x1	0.27	688.5	36	7250.83	24.72	0.96941176	293.3184	27.894	21.694	26.861	3209.47	0.00799	401685.86
x2	0.65	1657.5											
x1	0.29	739.5	36	7205.1	24.37	0.95568627	295.6545	28.253	22.048	27.426	3174.71	0.00857	370444.57
x2	0.62	1581											
x1	0.31	790.5	36	7230.7	24.46	0.95921569	295.6132	29.394	22.864	28.215	3197.81	0.00959	333452.55
x2	0.64	1632											
x1	0.32	816	36	7294.61	24.83	0.97372549	293.7821	30.301	23.429	28.85	3117.4	0.01027	303544.3
x2	0.68	1734											
x1	0.33	841.5	36	7275.22	24.75	0.97058824	293.9483	30.696	23.74	29.193	3147.88	0.0107	294194.39
x2	0.67	1708.5											
x1	0.35	892.5	36	7289.28	25.18	0.98745098	289.4869	31.719	24.467	30.076	3101.25	0.00895	346508.38
x2	0.68	1734											
x1	0.35	892.5	36	7399.13	26.32	1.03215686	281.122	31.608	24.33	30.376	3050.69	0.01224	249239.38
x2	0.73	1861.5											
x1	0.37	943.5	36	7325.73	26	1.01960784	281.7588	31.082	25.217	25.217	3072.75	0.0132	232784.09
x2	0.7	1785											

2.8 Numerical Results

The results of the 3D numerical analysis of the models of type (a) and type (b) were compared. The maximum displacements at the top of the models versus corresponding base shear forces of the models for both the types were categorized as capacity curves. The Capacity curves for both types of (a) and (b) are included two categories as similar and ultimate loading. The performance and stiffness of the models showed that, in the models of type (a), a model, which is located on the upper level of the diagrams, has more stiffness relative to other models. it was the model (0-0.55) H, that illustrated in Figure 6 and Figure 7. Consequently, regarding the optimized model of type (a), as the model (0-0.55) H with minimum top displacement by 34.55mm relative to values of the others models of this type (see Table 2).

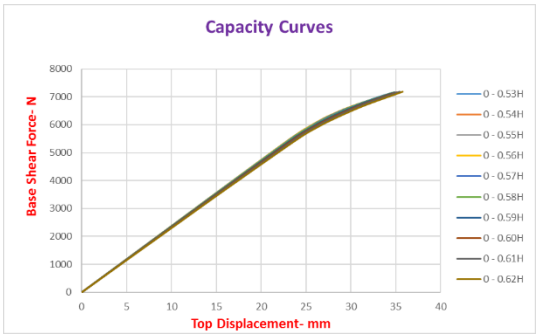

Figure 6: Type (a)- Similar loading 36KN/m^2

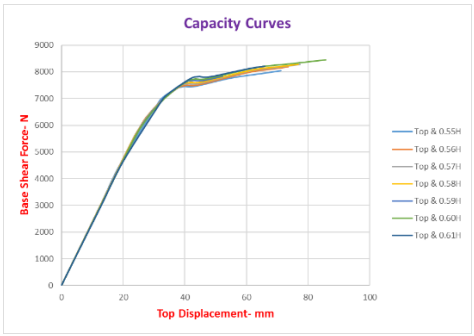

Figure 7: Type (a)- Ultimate loading ≥36KN/m^2

Thus, the model $(0.29 - 0.62)\ H$ of the models of type (b) was optimized with maximum reduction of displacement at the top of the building compared to others models in this type by 24.37mm (see Table 3). The capacity curves diagrams of this models for both loadings stages as shown by Figure 8 and Figure 9.

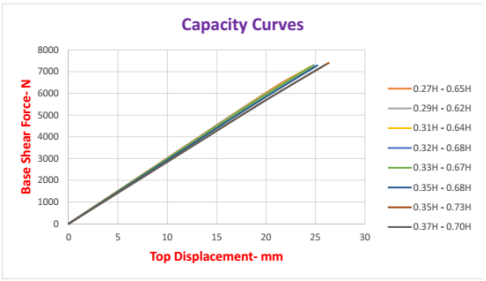

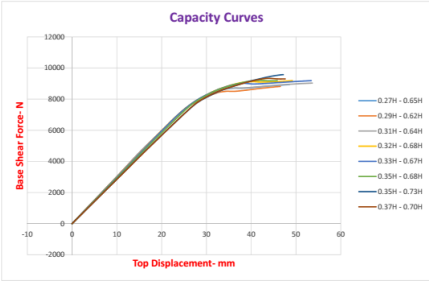

Figure 8: Type (b)- Similar loading 36KN/m^2 Figure 9: Type (b)- Ultimate loading ≥36KN/m^2

The yield stress value of the material properties was *168.11* Mpa and ultimate stress value was *203.17* Mpa, (see Table 1). The obtained results from the cantor's stress values from Abaqus /CAE 6.11 program showed that type (a) was failed by *217.64* Mpa and type (b) by *217.92 Mpa*. The stress value of the core as type (c) was *175.55* Mpa, compared to others types has less been stiffened that as shown bu Figure 10.

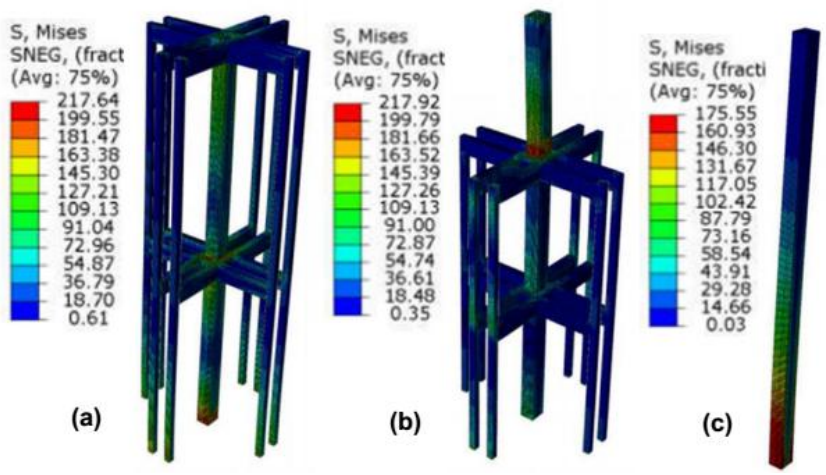

Figure 10: Cantor stress values of the failure modes: The model type (a), The model type (b) and (c) a single core alone

3.0 Conclusion

A comparison results of the 2D idealized analytical model with numerical results of the 3D models by Abaqus/CAE 6.11 program is presented. This is in relation to the efficiency of the two types of models (a) and (b) in the reduction of the lateral drift at the top of the building that were analyzed by two above mentioned methods. Optimum location of the outriggers to obtain optimum outriggered structure is presented and the decrease moment of the base of the structure was examined as well. The conclusions as follows:

1- The 2D analytical models, type of the model (a) in which, one outrigger is fixed at the top, the second outrigger was optimized at $0.58H$.

2- The 2D analytical models, type of the model (b) in which, both outriggers were optimized at $(0.31 - 0.69)\ H$.

3- The 3D numerical models, type of the model (a) in which, one outrigger fixed at the top, the second outrigger was optimized at $055H$.

4- The 3D numerical models, type of the model (b) in which, both outriggers were optimized at $(0.29 - 0.62)\ H$.

5- The 3D numerical models (FEA), efficiency in the reduction of the lateral displacement at the top of the structure by type of the optimized model (b) is *42%* higher than type of the optimized model (a).

6- The 3D numerical models (FEA), efficiency in the reduction of the base moment by type of the optimized model (b) is *24%* higher than type of the optimized model (a).

4.0 Acknowledgements

The author would like to thanks, Prof. Abdul Kadir Marsono for the outstanding support that he made for ensuring the quality of the work in Universiti Technologi Malaysia.

References

Alpana L. Gawate, J. P. B. (2015). behavior of outrigger structural system for high rise building. *International Journal of Modern Trends in Engineering and Research (IJMTER)*. 2(7).

ATC (1996). redwood city, California: applied technology council (report no 40).

Fawzia, S. and Fatima, T. (2010). Deflection control in composite building by using belt truss and outriggers system. *Proceedings of the 2010 Proceedings of the 2010 World Academy of Science, Engineering and Technology conference*,

FEMA-273 (1997). Washington D.C: developed by the building seismic safety council for the federal emergency management agency.

FEMA-356 (2000). *volume 1*. redwood city, California: applied technology council (report no 40).

Ghosh, S. K., Fanella, D. A. and Rabbat, B. G. (1996). *Notes on ACI 318-95, Building Code Requirements for Structural Concrete: With Design Applications*. Portland cement association.

Goel, R. K. (2005). Evaluation of modal and FEMA pushover procedures using strong-motion records of buildings. *Earthquake spectra*. 21(3), 653-684.

Günel, M. H. and Ilgin, H. E. (2014). *Tall Buildings: Structural Systems and Aerodynamic Form*. Routledge.

Herath, N., Haritos, N., Ngo, T. and Mendis, P. (2009). Behaviour of outrigger beams in high rise buildings under earthquake loads. *Proceedings of the 2009 Australian Earthquake Engineering Society 2009 Conference*,

Hoenderkamp, J. (2008). Second outrigger at optimum location on high- rise shear wall. *The structural design of tall and special buildings*. 17(3), 619-634.

Kamath, K., Divya, N. and Rao, A. U. (2012). A Study on Static and Dynamic Behavior of Outrigger Structural System for Tall Buildings. *Bonfring International Journal of Industrial Engineering and Management Science*. 2(4), 15.

Samat, R. A., Ali, N. M. and Marsono, A. K. (2008). The Optimum Location of Outrigger in Reducing the Along-Wind and Across-Wind Responses of Tall Buildings. *Malaysian Journal of Civil Engineering*. 20(2).

Smith, B. S. and Coull, A. (1991). *Tall building structures: analysis and design*. University of Texas Press.

Smith, B. S. and Salim, I. (1983). Formulae for optimum drift resistance of outrigger braced tall building structures. *Computers & Structures*. 17(1), 45-50.

Standard, A. (2004). E8-04,". *Standard Test Methods for Tension Testing of Metallic Materials," Annual Book of ASTM Standards*. 3.

Zeidabadi, N. A., Mirtalae, K. and Mobasher, B. (2004). Optimized use of the outrigger system to stiffen the coupled shear walls in tall buildings. *The structural design of tall and special buildings*. 13(1), 9-27.